CROSS SECTIONS FOR RADIATIVE CAPTURE OF NEUTRONS WITH ENERGIES UP TO 50 keV *BY* La^{139}, Pr^{141}, Ta^{181}, *AND* Au^{197}

V. A. KONKS, Yu. P. POPOV, and F. L. SHAPIRO

P. N. Lebedev Physics Institute, Academy of Sciences, U.S.S.R.

Submitted to JETP editor July 12, 1963

J. Exptl. Theoret. Phys. (U.S.S.R.) **46**, 80-88 (January, 1964)

Cross section curves for radiative capture of neutrons and data on resonance capture integrals obtained with a neutron-slowing-down-time spectrometer employing lead are presented. The values of the force functions for p neutrons (S_1) and of the quantities $S_\gamma = \Gamma_\gamma/\bar{D}_J(2J+1)$ are determined from an analysis of the energy dependences of the capture cross sections. For lanthanum $S_1 = (2.0 \pm 0.9) \times 10^{-4}$, $S_\gamma = (0.20 \pm 0.02) \times 10^{-4}$; for praseodymium $S_1 = (1.1^{+1.1}_{-0.6}) \times 10^{-4}$, $S_\gamma = (0.60 \pm 0.07) \times 10^{-4}$; for tantalum $S_1 \sim 0.2 \times 10^{-4}$; for gold $S_1 \sim 0.3 \times 10^{-4}$.

INTRODUCTION

THE energy region up to 50 keV is most favorable for observing interactions between p neutrons and nuclei, because s and p neutrons make comparable contributions to the capture cross section in this region, while the contribution of d neutrons is negligibly small.[1] While ample experimental information is available regarding the force functions for s neutrons, the force functions S_1 for p neutrons have been measured for only a relatively small number of nuclei, mainly in the region A $\sim$ 100,[1-3] where the function $S_1(A)$ reaches a maximum. In the region A $\sim$ 140—200, where our present measurements were made, S_1 has a minimum (and S_0 a maximum); this, of course, makes it difficult to distinguish the p-neutron contribution to capture cross sections averaged over many resonances. On the other hand, the experimental determination of S_1 in this region of A is of decided interest, particularly in connection with recent theoretical papers discussing volume and surface absorption in the optical model and the effect of nuclear deformation (see [4,5], for example).

Systematic measurements of the energy dependence of radiative neutron capture cross sections below 50 keV were begun only recently. Relative measurements of the cross sections were obtained above 3 keV for some nuclei at Duke University using the activation technique.[3] Measurements at Oak Ridge for $E \gtrsim 10$ keV[2] and $E < 8$ keV[6] employed the direct registration of prompt γ rays from neutron capture.

Capture cross sections of neutrons from an Sb–Be source (E = 24 keV) and of neutrons from the $Li^7(p,n)$ reaction near threshold (30 keV) have been measured using the activation technique[7-11] and by transmission with spherical geometry.[12,13] However, the spread of experimental results obtained by different investigators is still quite large; gold is a good example in this respect.

Our present measurements represent a continuation of previous work.[14] We used a spectrometer based on the neutron slowing-down time in lead.[14-16]

RESULTS

Our measurements of the energy dependence of neutron radiative capture cross sections give the relative variation of the cross sections and can be normalized in three different ways:[14]

1) to the known resonance parameters of low-lying levels of the investigated elements;

2) to the cross section for thermal neutron capture;

3) to known resonance parameters of a different element.

Lanthanum. Measurements were made with three thicknesses ($\bar{n} = 1.5 \times 10^{21}$, 3.4×10^{21}, and 8×10^{21} atoms/cm^2) of samples from three batches of lanthanum oxide. The capture cross section was normalized to the 73.5-eV resonance level of lanthanum,[17] and also to the resonances of gold, tantalum, and tungsten in simultaneous measurements (Table I).

Figure 1 shows the energy dependence of the capture cross section for lanthanum. For E > 1 keV measurements with samples of different thicknesses yielded identical results. Measurements revealed the level $E_0 = 3.06$ of La^{138} (0.089% of a natural mixture); the known 0.752-eV level of

Table I. Calibration coefficients K of separate series of measurements for lanthanum, praseodymium, tantalum, and gold

Normalization	K	Normalization region, eV	K
Lanthanum, $\bar{n} = 4.7 \times 10^{21}$ atoms/cm²		Tantalum, $\bar{n} = 4.6 \times 10^{21}$ atoms/cm²	
to $E_0 = 73$ eV level of La^{139}	0.047±0.008	to 7.2	0.076±0.005
to tungsten	0.035±0.004	7.2—16	0.065±0.003
to gold	0.043±0.009	16—55	0.077±0.002
to tantalum	0.041±0.004	0.3	0.072±0.004
Praseodymium, $\bar{n} = 8 \times 10^{21}$ atoms/cm²		Gold, $\bar{n} = 1.7 \times 10^{21}$ atoms/cm²	
to $E_0 = 85$ eV level of Pr^{141}	0.038±0.006	to 36	0.186±0.008
to tungsten	0.036±0.004	36—110	0.184±0.015
to bromium	0.039±0.008	110—220	0.162±0.011
to tantalum	0.040±0.004	0.3	0.189±0.010

Note. The indicated error limits were based on errors in the employed resonance parameters, and in the low-energy calibration on the statistical accuracy and stability of the measurements.

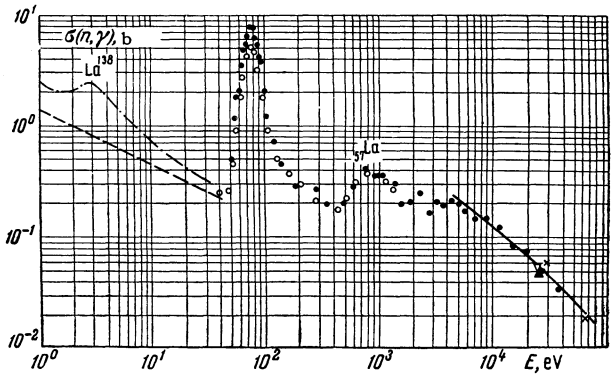

FIG. 1. Energy dependence of neutron capture cross section for lanthanum samples with $\bar{n} = 3.4 \times 10^{21}$ atoms/cm² (●) and $\bar{n} = 8.0 \times 10^{21}$ atoms/cm² (○). – our data; × from [2]; ▽ from [7]; ▼ from [8]. Dashed straight line–1/v extrapolation of the thermal capture cross section; [17] dash-dot curve–experimental; continuous curve (in keV region)–capture cross section plotted from the parameters S_1 and S_2 given in the text and $S_0 = 2 \times 10^{-4}$.

La^{139} was weak. Below 10 eV the capture cross section of lanthanum is approximately twice as large as the thermal neutron capture cross section extrapolated according to the 1/v law; this cannot be accounted for entirely by the indicated low-lying levels of La^{138} and La^{139}. The enhanced cross section, as in the case of praseodymium (see below), is evidently accounted for by admixtures of other rare earth elements. However, the maximum cross section at ~ 800 eV cannot be explained by such admixtures, but corresponds to a group of narrow lanthanum resonances not appearing in the measurements of the total cross sections. [17]

Below 10 keV our measurements are in good agreement with results reported in [2,7,8].

Praseodymium. Measurements were performed on three thicknesses of samples from two batches of a complex oxide. The uncertain composition of the latter led to an error of at most 2% in determining the mean sample thickness when the calculation was based on the formula Pr_6O_{11}.

Figure 2 illustrates the relation between the measured effect and the background for a praseodymium sample with $\bar{n} = 4.2 \times 10^{21}$ atoms/cm² measured with a proportional γ counter.

Figure 3 shows the capture cross section as a function of neutron energy. The cross sections were normalized to the resonance parameters of Pr^{141} at $E_0 = 85$ eV,[1)] and also to the resonance parameters of Br, Ta, and W. The agreement with the calibration coefficients is seen in Table I.

Below 10 keV the measured cross section lies above the cross section representing 1/v extrapolation from the thermal region (dash-dot curves 1 and 2). This result at low energies is caused by an admixture of such rare earth elements as Sm, Gd, Dy, and Eu. (To account for the observed behavior of the capture cross section we require only 0.05—0.1% of each of these elements; the impurity analysis was not performed with this degree of accuracy.) Measurements on samples from two different batches of praseodymium oxide yielded different cross section curves at low energies. On

[1)] It should be noted that the parameters of the 85-eV resonance from [19] and the measurements of L. B. Pinkel'ner, Yu. S. Yazvitskii et al. were close, whereas those of other authors [17] differed greatly. We used the data of Pinkel'ner et al. The calibration coefficient K for the group of levels in the region 150–300 eV was weighted 1/2 because of the large correction for neutron capture after scattering, which was calculated with considerable error. [20]

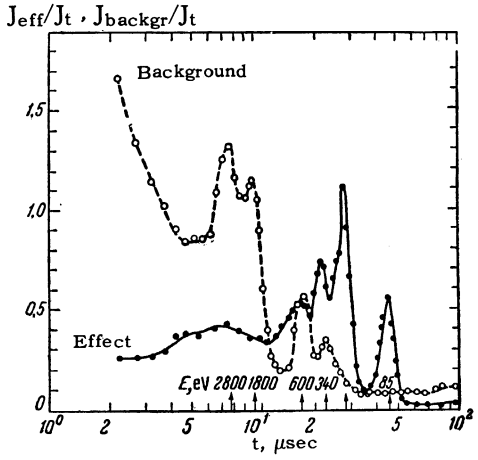

FIG. 2. Curves of the measured effect and background, for a thin praseodymium sample, as a function of slowing-down time.

curve 2 a level appears at ~ 8 eV, which can be associated with the strong 8.01-eV level of Sm^{152}. In the case of the other batch of praseodymium a group of levels was noted having the mean energy ~ 6 eV, which can be attributed to dysprosium (curve 1). The areas of the peaks correspond to Sm and Dy contents of the order of tenths of one percent. Agreement with the results given by other authors [2,7,8] is satisfactory in the keV region.

Tantalum. Measurements were performed on two sheet tantalum samples of different thicknesses and on a sample of powdered tantalum from a different batch. The cross sections were normalized to levels with known resonance parameters [21,22] and to the thermal capture cross section (Table I). The energy dependence of the radiative neutron capture cross section for tantalum is shown in Fig. 4; a comparison of the results for three sample thicknesses shows the self-shielding effect. At energies above ~ 2 keV the points for samples of different thicknesses are averaged, since self-shielding no longer plays a part in this region. Below ~ 0.5 eV the neutron capture cross section of tantalum follows the 1/v law. Our results are in good agreement with [2,6]. Above 20 keV our data are 25% lower than in [8,23].

Gold. Two metallic gold samples of different thicknesses were used. The capture cross section was normalized to resonance levels with known parameters [21] and to the thermal capture cross section. [17]

Table I gives calibration coefficients for one series of measurements on gold. The weighted mean calibration coefficient was used for normal-

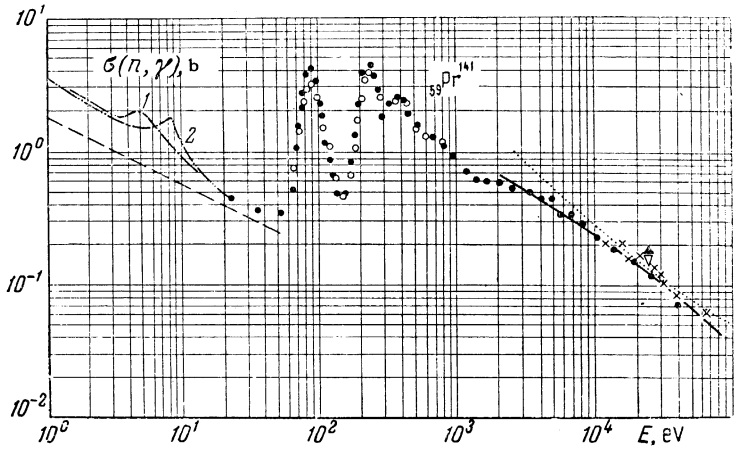

FIG. 3. Energy dependence of neutron capture cross section for praseodymium samples with $\bar{n} = 4.2 \times 10^{21}$ atoms/cm² (●) and $\bar{n} = 10^{22}$ atoms/cm² (○). – our data; × from [2]; ▲ from [8]; ▽ from [18]. Dashed straight line at low energies–1/v extrapolation of the thermal capture cross section;[18] dash-dot curves 1 and 2–experimental for samples from different batches of praseodymium oxide; continuous curves(in keV region) –capture cross section plotted from the parameters in the text with $S_0 = 2 \times 10^{-4}$; dotted curve–analogously using the parameters in [2].

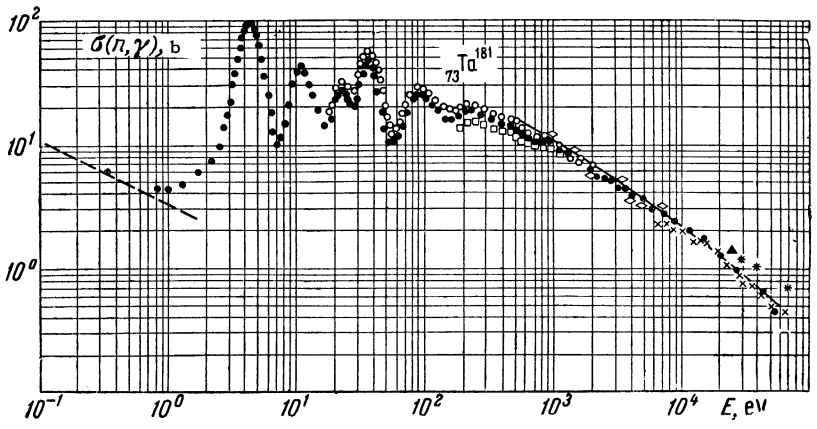

FIG. 4. Energy dependence of neutron capture cross section for tantalum samples with $\bar{n} = 2.8 \times 10^{21}$ atoms/cm² (○), $\bar{n} = 4.6 \times 10^{21}$ atoms/cm² (●), and $\bar{n} = 8.7 \times 10^{21}$ atoms/cm² (□). × from [2]; ◇ from [6]; ▲ from [8]. * from [23]. Dashed and continuous curves as in Fig. 1.

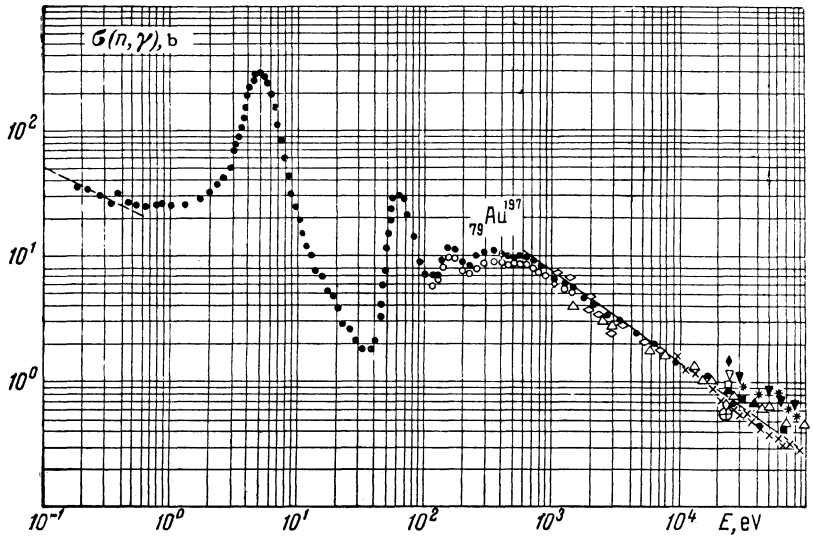

FIG. 5. Energy dependence of neutron capture cross section for gold samples with $\bar{n} = 2 \times 10^{21}$ atoms/cm^2 (○) and $\bar{n} = 4 \times 10^{21}$ atoms/cm^2 (●). × from [2]; △ from [3]; ◇ from [6]; ▽ from [7]; ▲ from [8]; ◆ from [9]; ■ from [10]; □ from [11]; ⊕ from [12]; ◇ from [13]; * from [23]; ▽ from [25]. Curves as in Fig. 1.

ization. Earlier measurements[24] were normalized to resonance parameters given in [17]. The renormalization of old results to resonance parameters in [21] lowered the cross section curve 20%, giving agreement with our measurements within experimental error limits.

The energy dependence of the (n, γ) cross section for gold is shown in Fig. 5, taking account of the renormalized results in [24]. In the keV region our results agree well with [2,12,13,6]. Disagreement is observed with results in [7-11,25] obtained by the activation technique, and the shape of the curve differs from that obtained at Duke University.[3]

In Table I the calibration coefficients for gold in connection with the third resonance group and for tantalum in connection with the second group are 10—15% smaller than the other coefficients. This difference reappeared in all other series of measurements with samples of unequal thicknesses. The explanation may lie either in inaccurate parameters of these levels, obtained from total cross section measurements in [17,21,22], or in the omission by the same investigators of weak resonances making an appreciable contribution to the capture cross section.

It should also be noticed that for gold and tantalum a systematic discrepancy is observed between the activation data, on the one hand, and data obtained in the direct registration of γ quanta from neutron capture and by neutron transmission with spherical geometry, on the other hand. The activation data for gold[7-11,23,25] exhibit a considerable amount of mutual discrepancy and are one and one-half to two times higher than the results in [2,12,13] and our own data, which are in good mutual agreement. Since gold and tantalum have strong resonances at low energies, it is possible that the presence of even a small low-energy neutron background (reflected from room walls etc) leads to a spurious increase of the capture cross section for activation.[2)] A change of the decay scheme upon passing from the thermal region (to which these measurements were normalized) to the keV region can only lead to the appearance of new decay modes which would reduce the measured cross section in the keV region, and not the reverse.

In connection with the design of nuclear reactors and radiation shielding it is of interest to consider the resonance absorption integral

$$R_\gamma = \int_{E_1}^{E_2} \sigma_\gamma(E) \frac{dE}{E}.$$

Table II gives R_γ in different energy regions. Here $R_\gamma(1/v) = 0.44\,\sigma_\gamma(0.025\ \text{eV})$, R_1 was calculated from the parameters of known resonances, and R_1 was obtained from our measurements on the thinnest sample for the energy region (given in parentheses) where the parameters of the levels were unknown. The total value of R_γ is given in the fifth column. The sixth column gives values of R_γ obtained by other investigators mainly from reactor measurements. In the cases of gold and tantalum R_γ was determined practically entirely from the value of R_1, not from our measurements; therefore a comparison with other "global" values of R_γ would be meaningless.

[2)] It is therefore necessary to perform activation measurements for nuclei with strong low-lying resonances using screens of the same elements as shields against background neutrons.

Table II. Resonance absorption integrals

Element	R_γ (1/v), barn	R_1, barn	R_2, barn	Total R_γ, barn	R_γ, barn (other authors)
La	3.9±0.1	9.2±0.9 (<730 eV)	0.9±0.1 (>730 eV)	14.0±0.9	11[26]; 11±3[27]
Pr	4.97±0.09	9.7±0.7 (<300 eV)	2.9±0.3 (>300 eV)	17.6±0.8	11.3[26]; 23.5±9 [27]
Ta *	9.23±0.44		12.6±1.3 (>1 keV)		
Au *	43.5±0.1		9.6±0.9 (>1 keV)		

*Very accurate resonance parameters of Ta levels up to 300 eV and of Au levels up to 940 eV are given in [21].

We shall finally discuss the force functions for p neutrons which were calculated from the average capture cross sections in lanthanum, praseodymium tantalum, and gold. These calculations followed a program developed in [1]. However, the small contribution of p neutrons to the capture cross section reduces considerably the reliability of the S_1 calculation, so that more rigorous accuracy is required for the s-neutron average interaction parameters. The initial calculations showed the impossibility of obtaining the three parameters from our curves (the second and third series of calculations in [1]). Moreover, in the cases of tantalum and gold we do not obtain completely unique values of the two parameters S_1 and $S_\gamma = \overline{(\Gamma_\gamma/D)_0} = \overline{(\Gamma_\gamma/D)_1}$ (here $D = D_J(2J+1)$, where D_J is the average separation between levels with spin J). A change of 15—20% from the fixed value of the force function for s neutrons (the error of S_0 indicated in one of the best references [21]) changes S_1 by a factor of a few. For the given elements our measurements yield only estimates of S_1 (0.2×10^{-4} for tantalum and 0.3×10^{-4} for gold). These estimates agree with [2,3].

It should also be noted that our experimental capture cross sections for gold and tantalum in the range ~ 1—4 keV are 15—20% higher than the results calculated using values of S_0 and S_γ given in [21].

For La^{139} and Pr^{141}, which are magic nuclei for neutrons, we have $\overline{\Gamma}_n \gg \Gamma_\gamma$ above 3 keV. Therefore the s-neutron capture cross section averaged over resonances depends mainly on $\Gamma_\gamma/\overline{D}$ (as is discussed more fully in [1]). An analysis of the measurements therefore gives $\overline{\Gamma_\gamma/D}$ with greater accuracy than S. Assuming $\overline{(\Gamma_\gamma/D)_0} = \overline{(\Gamma_\gamma/D)_1} = S_\gamma$, we obtain:

for lanthanum $S_\gamma = (0.20 \pm 0.02)\cdot 10^{-4}$,

$S_1 = (2 \pm 0.9)\cdot 10^{-4}$;

for praseodymium $S_\gamma = (0.60 \pm 0.07)\cdot 10^{-4}$,

$S_1 = \left(1.1\ {}^{+1.1}_{-0.6}\right)\cdot 10^{-4}$.

The last value is one order of magnitude greater than the result $S_1 = (0.1 \pm 0.1) \times 10^{-4}$ given in [2]. Figure 3 shows the capture cross section curves of praseodymium calculated from our parameters (the continuous curve) and from the parameters in [2] (dotted curve). It can be seen that the latter disagrees with experiment below 10 keV. This results from the fact that Gibbons et al.[2] used the higher value $S_\gamma = 1.1 \times 10^{-4}$. In the region above 100 keV, which is not shown in Fig. 3, the experimental points lie above our calculated curve. This can be accounted for by the contribution of d neutrons, whose force function should have a maximum at $A \approx 140$.[28]

It may be noted that the values of S_1 obtained for lanthanum and praseodymium agree with those calculated on the optical model using the parameters of Nemirovskiĭ[28] (see [1] also).

In conclusion the authors wish to thank Yu. A. Dmitrenko, S. N. Gubernov, A. M. Klabukov, and E. D. Bulatov for maintaining the proper functioning of the apparatus, and Yu. I. Fenin for the computer calculations.

[1] Yu. P. Popov and Yu. I. Fenin, JETP **43**, 2000 (1962), Soviet Phys. JETP **16**, 1409 (1963).

[2] Gibbons, Macklin, Miller, and Neiler, Phys. Rev. **122**, 182 (1961).

[3] Bilpuch, Weston, and Newson, Ann. Phys. **10**, 455 (1960); Weston, Seth, Bilpuch, and Newson, Ann. Phys. **10**, 477 (1960).

[4] Yu. P. Elagin, JETP **44**, 371 (1963), Soviet Phys. JETP **17**, 253 (1963).

[5] B. Buck and F. Perey, Phys. Rev. Letters **8**, 444 (1962).

[6] Block, Slaughter, Weston, and Vonderlage, Neutron Time of Flight Methods, Brussels, 1961, p. 203.

[7] Macklin, Lazar, and Lyon, Phys. Rev. **107**, 504 (1957).

[8] Booth, Ball, and MacGregor, Phys. Rev. **112**, 226 (1958).

[9] V. Hummel and B. Hamermesh, Phys. Rev. **82**, 67 (1951).

[10] L. W. Weston and W. S. Lyon, Phys. Rev. **123**, 948 (1961).

[11] Kononov, Stavisskiĭ, and Tolstikov, Atomnaya Énergiya **5**, 564 (1958), Sov. J. Atomic Energy **5**, 1483 (1958).

[12] H. W. Schmitt and C. W. Cook, Nuclear Phys. **20**, 202 (1960).

[13] T. S. Belanova, Atomnaya Énergiya **8**, 549 (1960), Soviet J. Atomic Energy **8**, 162 (1960).

[14] Yu. P. Popov and F. L. Shapiro, JETP **42**, 988 (1962), Soviet Phys. JETP **15**, 683 (1962).

[15] Bergman, Isakov, Murin, Shapiro, Shtranikh, and Kazarnovskiĭ, Proc. of the First International Conference on the Peaceful Uses of Atomic Energy, Geneva, 1956, IV, P/642, United Nations, N.Y.

[16] Kashukeev, Popov, and Shapiro, Neĭtronnaya fizika (Neutron Physics), Atomizdat, 1961, p. 353; J. Nuclear Energy **A14**, 76 (1961).

[17] D. J. Hughes and R. B. Schwartz, Neutron Cross Sections, BNL-325, 2. ed., 1958; Hughes, Magurno, and Brussel, Neutron Cross Sections, BNL-325 Suppl. 1, 1960.

[18] W. S. Lyon and R. L. Macklin, Phys. Rev. **114**, 1619 (1959).

[19] Corge, Huynh, Julien, Morgenstern, and Netter, J. phys. radium **22**, 719 (1961).

[20] J. E. Draper, Nuclear Sci. Eng. **1**, 522 (1956).

[21] Desjardins, Rosen, Havens, and Rainwater, Phys. Rev. **120**, 2214 (1960).

[22] Doil'nitsyn, Khamyakov, and Parfenov, Materials of a Working Conference on Neutron Physics, Preprint, Joint. Inst. Nuclear Res. No. 956, 1962, p. 52.

[23] Miskel, Marsh, Lindner, and Nagle, Phys. Rev. **128**, 2717 (1962).

[24] Isakov, Popov, and Shapiro, JETP **38**, 989 (1960), Soviet Phys. JETP **11**, 712 (1960).

[25] S. A. Cox, Phys. Rev. **122**, 1280 (1961).

[26] R. L. Machlin and H. S. Pomerance, op. cit.[15], V, P/833.

[27] J. D. Garrison and B. W. Roos, Nuclear Sci. Eng. **12**, 115 (1962).

[28] P. É. Nemirovskiĭ, Sovremennye modeli atomnogo yadra (Modern Nuclear Models), Atomizdat, 1960.

Translated by I. Emin
11